adhesion between surfaces. The method described here, which is based on deformations in a compliant polymeric lens and sheet, is sensitive to small variations in the compositions of the surface. In terms of analyzing surface energetics, it is complementary to measuring contact angles. Although we have so far studied systems that interact primarily through London–van der Waals forces, the method can also be used to investigate more complex interfacial interactions (for example, hydrogen bonding) by incorporating relevant functional groups on the surface of the PDMS (*25*).

REFERENCES AND NOTES

1. W. A. Zisman, *Adv. Chem. Ser.* **43**, 1 (1964).
2. T. Young, *Miscellaneous Works*, G. Peacock, Ed. (Murray, London, 1855), p. 1.
3. L. A. Girifalco and R. J. Good, *J. Phys. Chem.* **61**, 904 (1957); R. J. Good and L. A. Girifalco, *ibid.* **64**, 561 (1960); F. M. Fowkes, *Ind. Eng. Chem.* **56**, 40 (1964). The theories of intermolecular forces for dispersive systems only predict that the energy of intermolecular interaction between dissimilar phases is given by the geometric mean of their cohesive energies of interaction. Stretching this conclusion to surface free energies (as has been done with Eq. 2) has never been justified theoretically. Therefore Eq. 2 is semiempirical.
4. In his classic paper (*1*), Zisman wrote: "Unfortunately, the effect of constitution on either $\gamma_{SV}{}^0$ or γ_{SL} is still unknown, and neither quantity can be studied until a satisfactory experimental method for measuring it has been found . . ." (Note that the symbol $\gamma_{SV}{}^0$ in this statement has, basically, the same physical meaning as that of γ_{SV}; the superscript "0" implied that the measurements are made under saturated vapor pressure.) One major experimental difficulty in analyzing the energetics of solid surfaces arises because most real systems exhibit hysteresis of some sort, indicating that they are not at thermodynamic equilibrium. Young's equation strictly applies only at equilibrium.
5. K. L. Johnson, K. Kendall, A. D. Roberts, *Proc. R. Soc. London Ser. A* **324**, 301 (1971). Significant contributions to our understanding of the deformations between elastic solids were also made by the school of Derjaguin *et al.* [B. V. Derjaguin, *Kolloid Z.* **69**, 155 (1934); ______, V. M. Muller, Yu. P. Toporov, *J. Colloid Interface Sci.* **53**, 314 (1975)]. However, JKR theory is more applicable for our present purpose (*12*). See (*6*) for the details describing the differences between various theories dealing with contact deformations.
6. R. G. Horn, J. N. Israelachvili, F. Pribac, *J. Colloid Interface Sci.* **115**, 480 (1987).
7. K. Kendall, *J. Phys. D* **4**, 1186 (1971); *J. Adhesion* **5**, 77 (1973).
8. D. Maugis and M. Barquins, *Adhesion and Adsorption of Polymers: Polymer Science and Technology*, L. H. Lee, Ed. (Plenum, New York, 1980), vol. 12A, p. 203; M. Barquins and R. Courtel, *Wear* **32**, 133 (1975).
9. A. D. Roberts and A. B. Othman, *Wear* **42**, 119 (1977).
10. D. Tabor, *J. Colloid Interface Sci.* **58**, 2 (1977).
11. A. E. Lee, *ibid.* **64**, 577 (1978).
12. M. K. Chaudhury and G. M. Whitesides, *Langmuir* **7**, 1013 (1991).
13. G. S. Ferguson, M. K. Chaudhury, G. B. Sigal, G. M. Whitesides, *Science* **253**, 776 (1991).
14. J. Sagiv, *J. Am. Chem. Soc.* **102**, 92 (1980); R. Maoz and J. Sagiv, *J. Colloid Interface Sci.* **100**, 465 (1984); S. R. Wasserman, Y.-T. Tao, G. M. Whitesides, *Langmuir* **5**, 1074 (1989); N. Tillman, A. Ulman, J. S. Schildkraut, T. C. Penner, *J. Am. Chem. Soc.* **110**, 6136 (1988).
15. The original JKR equation was expressed in terms of *W*, the work of adhesion. For two similar surfaces, *W* is equal to $2\gamma_{SV}$, and thus we have expressed the JKR equation in terms of γ_{SV}.
16. The conditions used for silanization of PDMS^{ox} were slightly different from those reported in (*12*). Under new conditions, desiccators containing paraffin oil solutions of silanes were evacuated to about 0.001 torr for 30 min. Oxidized PDMS samples were usually placed at about 1.5 cm from the oil level. The concentrations of silanes were 60 μl of silane per 3 g of paraffin oil, except for the fluoroalkylsilane for which the concentration was 5 μl silane per 3 g of paraffin oil. We could consistently obtain surfaces exhibiting low hysteresis using these conditions.
17. The exact nature of the plasma-oxidized surface of PDMS is unclear. Most reports, however, agree that it contains silanol groups. For examples, see: D. W. Fakes, M. C. Davies, A. Brown, J. M. Newton, *Surf. Interface Anal.* **13**, 233 (1988); D. W. Fakes, J. M. Newton, J. M. Watts, M. J. Edgell, *ibid.* **10**, 416 (1987); M. Morra *et al.*, *J. Colloid Interface Sci.* **137**, 11 (1990). The findings of Fakes *et al.* indicated that the structure of the surface resembles that of inorganic silica. Morra *et al.* believe that the structure is more complex. The formation of surface silanols is, however, widely accepted. The surface properties of the silane-treated PDMS^{ox} are, however, determined by the composition and structure of the silane, not by the underlying oxide layer (*12, 13*). The wettability properties of the silane-treated PDMS^{ox} surfaces are similar to those of the corresponding monolayers formed on silicon wafer.
18. The methyl ether surface, when freshly formed, exhibited significant hystereses in both contact angles and contact deformations (not reported here). It was necessary to rinse this surface in decalin, ethanol, and water in order to minimize hysteresis.
19. The load-deformation and contact-angle measurements were performed on different samples taken from the same batch.
20. The origin of the large hysteresis of diiodomethane on the fluorocarbon surface is not clear. Because of the high hysteresis, we did not use this liquid to calculate γ_{SV} of the fluorocarbon surface.
21. Similar anomalies in the values of γ_{SV} for the fluorocarbon and hydrocarbon surfaces (as estimated using contact angles) have also been observed by Fowkes [F. M. Fowkes, *Adv. Chem. Ser.* **43**, 99 (1964)]. Non-ideal interaction between fluorocarbons and hydrocarbons is also well known in their solubility properties [see J. H. Hilderbrand and R. L. Scott, *Solubility of Non-Electrolytes* (Reinhold, New York, ed. 3, 1950)].
22. These differences cannot be explained on the basis of the surface swelling because neither hexadecane nor diiodomethane swells monolayer-coated PDMS.
23. C. D. Bain and G. M. Whitesides, *J. Am. Chem. Soc.* **110**, 334 (1988). The term "high surface sensitivity" is used here loosely. Whether the liquids (water, glycerol, or diiodomethane) sense the underlying functional groups by long-range forces or by perturbing the structure of the surface is not clear.
24. High surface sensitivity of adhesion has also been demonstrated recently by Burnham *et al.* [N. A. Burnham, D. D. Dominguez, R. L. Mowery, R. J. Colton, *Phys. Rev. Lett.* **64**, 1931 (1990)], who used an atomic force microscope to measure the force between tungsten and different surfaces, including Langmuir-Blodgett films of stearic acid and ω,ω,ω-trifluorostearic acid deposited on Al/Al_2O_3. In these studies the adhesion force between tungsten and monolayer-coated alumina changed remarkably when the surface composition varied from $-CH_3$ to $-CF_3$.
25. M. K. Chaudhury, unpublished results.

26. M.K.C. acknowledges support from Dow Corning. The initial stages of this work at Harvard University were supported in part by the Office of Naval Research and the Defense Advanced Research Projects Agency. We thank M. J. Owen (Dow Corning) for many valuable discussions.

3 October 1991; accepted 9 January 1992

Dissociation of Individual Molecules with Electrons from the Tip of a Scanning Tunneling Microscope

G. DUJARDIN, R. E. WALKUP, PH. AVOURIS

The scanning tunneling microscope (STM) can be used to select a particular adsorbed molecule, probe its electronic structure, dissociate the molecule by using electrons from the STM tip, and then examine the dissociation products. These capabilities are demonstrated for decaborane(14) ($B_{10}H_{14}$) molecules adsorbed on a silicon(111)-(7 × 7) surface. In addition to basic studies, such selective dissociation processes can be used in a variety of applications to control surface chemistry on the molecular scale.

THE SCANNING TUNNELING MICROSCOPE (STM) can be used to control the structure and properties of materials on surfaces at the atomic or molecular level. The STM has been previously used to transfer clusters of atoms from the STM tip to the sample (*1*), to write molecular-scale marks on graphite (*2*), to reposition adsorbed atoms and molecules on metal surfaces (*3, 4*), and to reversibly transfer individual atoms between a surface and a tip by the application of voltage pulses (*4–6*). At a somewhat more macroscopic level, the STM has been used for a variety of nanometer-scale surface modifications (*7, 8*), including the deposition and etching of materials on surfaces, the electron-stimulated desorption of adsorbates (*9*), and the exposure of lithographic films using the STM tip as a field-emission electron source (*10*). In this report, we discuss the dissociation of individual adsorbed molecules using low-energy electrons from the tip. With the STM, one can select a particular adsorbed molecule, probe its electronic structure, dissociate the molecule, and then examine the dissociation products.

We investigated decaborane (14)

G. Dujardin, Laboratoire de Photophysique Moleculaire, Bâtiment 213, Université Paris-Sud, 91405 Orsay, France.
R. E. Walkup and Ph. Avouris, IBM Research Division, IBM Thomas J. Watson Research Center, Yorktown Heights, NY 10598.

($B_{10}H_{14}$) adsorbed on the Si(111)-(7 × 7) surface. This system offers a number of experimental advantages. Decaborane(14) has a vapor pressure of $\sim 10^{-1}$ torr at room temperature (*11*) and can be used as a convenient source of boron for surface reactions. Because of an interest in achieving precise control over the doping of Si with B, the adsorption and decomposition of $B_{10}H_{14}$ on Si surfaces has been studied with a variety of surface-science techniques (*12–16*). $B_{10}H_{14}$ adsorbs on the Si(111)-(7 × 7) surface at room temperature and can be directly imaged with the STM (*13*), and it can be readily decomposed by low-energy electrons (*16*). The STM used in our studies is mounted in an ultrahigh vacuum chamber (base pressure $<1 \times 10^{-10}$ torr). Details of the apparatus and sample preparation techniques are described elsewhere (*17*).

In each set of experiments, a clean Si(111)-(7 × 7) surface was prepared and examined with the STM. Topographic images (Fig. 1A) were obtained with the Si sample biased to +2 V with respect to the tip and with a constant tunneling current of ~200 pA. After imaging the clean surface, a small dose of $B_{10}H_{14}$ was admitted to the vacuum chamber, typically ~0.01 L (1 L = 10^{-6} torr s). Upon exposure at room temperature, molecules could be detected on the surface, as previously reported (*13*).

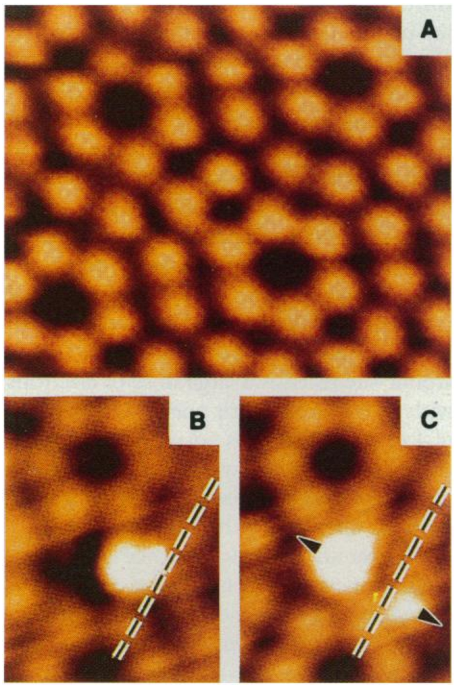

Fig. 1. (**A**) An STM image of the clean Si(111)-(7 × 7) surface with the sample biased to +2 V. (**B**) An isolated $B_{10}H_{14}$ molecule (large white spot) adsorbed next to a dark defect. (**C**) The result of electron bombardment at a bias voltage of +8 V. A large molecular species is now located over the original defect, and an additional fragment (small white spot) is seen to the lower right. The lateral distance between the large dark "corner holes" of the Si surface is 27 Å, and the color scale indicates a vertical range of 1 Å from black to white.

For low exposures of $B_{10}H_{14}$ (~0.01 L), isolated molecules generally adsorbed near defects on the surface (Fig. 1B). Preferential adsorption near defects indicates that $B_{10}H_{14}$ is initially in a mobile precursor state. Note that the STM can image only those molecules that are not mobile over the course of a measurement (~1 s). At higher exposures (~0.1 L), $B_{10}H_{14}$ was observed to adsorb over a variety of sites on the (7 × 7) surface, with a propensity for adsorption over center Si adatoms. We observed molecules with two different apparent sizes, with comparable populations in each size group. Molecules of one size group appear to be larger in images taken at positive bias voltages, but smaller at negative biases. We believe that the two size groups correspond to distinct adsorption geometries of the same molecular species because during some topographic scans conversion from one size to the other was observed. With the exception of an infrequent conversion as mentioned above, the adsorbed molecules could be reproducibly imaged at ±2 V with a ~200-pA tunneling current. In all of the images taken at ±2 V, the adsorbed molecules appear as protrusions from the surface, with a width of ~7 Å and a height of ~2 Å. For comparison, isolated $B_{10}H_{14}$ molecules have a major diameter of ~7 Å. With the STM we observe only the overall shape of the molecule; individual B–H bonds are not resolved.

Some insight into the bonding of the molecule to the surface can be gained by probing the valence electronic structure with scanning tunneling spectroscopy. In this technique, the tunneling current is measured as a function of bias voltage, while a topographic image is simultaneously recorded. Within a simple model of the tunneling process (*18*), the differential conductance dI/dV would be proportional to the local density-of-states of the sample if the tip has a constant density of electronic states. In practice, the tip electronic structure often plays an important role (*19, 20*), so that the correspondence between experimental dI/dV curves and the sample density-of-states is only qualitative. In Fig. 2 we show plots of dI/dV recorded with the STM tip positioned directly over an adsorbed molecule (solid curve) and over an Si adatom (dotted curve). These curves were recorded with the same tip during a single scan. Compared to the Si substrate, the adsorbed molecule has a small differential conductance for bias voltages in the range of −1 to +1 V, that is, the adsorbed molecule is effectively an insulator with a ~2-eV gap. The differential conductance strongly increases over the molecule for bias voltages >1 V or <−1 V. Although the detailed shapes of the dI/dV curves were tip dependent, the general features mentioned above were always present in the data.

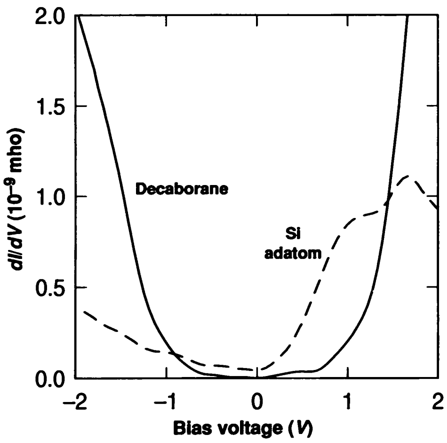

Fig. 2. The differential conductance (dI/dV) is shown for tunnel junctions with the STM tip positioned directly over a $B_{10}H_{14}$ molecule (solid curve) and over an Si adatom (dashed curve).

The conductance versus bias voltage relation has an important implication for molecular imaging. If one attempts to image the adsorbed molecules at low bias voltages ($|V_{\text{bias}}| < 1$ V), then the tip would displace toward the molecule during the scan in order to maintain a constant tunneling current. This movement may result in mechanical contact between the tip and the molecule and can cause displacement, reaction, or fragmentation of the molecule. However, for bias voltages of ±2 V, the molecular conductance is high, and thus the tip retracts as it scans over the molecule, and stable, reproducible imaging can be achieved.

The dI/dV measurements suggest that there is a substantial density of states associated with the adsorbed molecule, both on the occupied side ~1.5 eV below the Fermi level and on the unoccupied side ~1.5 eV above the Fermi level. In isolated $B_{10}H_{14}$ molecules, the occupied states are more strongly bound, ≃10 eV below the vacuum level (*21*). Thus the features observed on the dI/dV curves must arise from the chemisorption process. The $B_{10}H_{14}$ molecule can react (*22*) by donating a proton to a nearby site, thus forming the $(B_{10}H_{13})^-$ anion. Alternatively, $B_{10}H_{14}$ may react by loosing two hydrogen atoms and then binding to two ligands that act as electron donors (*22*). In either case the boron-hydride cage takes on an anionic form with occupied states that are less strongly bound than those of $B_{10}H_{14}$, in qualitative agreement with the observed dI/dV curves.

After selecting a particular adsorbed molecule, we used the STM tip as a source of low-energy electrons to probe for electron-induced reactions. A large current density is delivered to the sample in this way; a 100-pA current distributed over a $\sim$100 Å^2 region corresponds to $\sim 10^6$ electrons passing through each atomic site per second. For our scanning parameters, an adsorbed molecule receives a dose of $\sim 10^5$ electrons during a single scan. The energy of the electrons can be controlled by adjusting the bias voltage between the sample and the tip, which is nominally at ground potential. As the bias voltage is increased from zero, the mechanism of current flow changes from tunneling to field emission. In the field emission regime, the kinetic energy of electrons incident upon the sample surface is generally taken to be the bias voltage minus the sample work function. However, the maximum available energy for an electron-induced inelastic process is somewhat greater because the final state of the electron could be at the bottom of the conduction band, rather than at the vacuum level. Thus, the tip provides a rather broad spectrum of available energies, limited by the bias voltage.

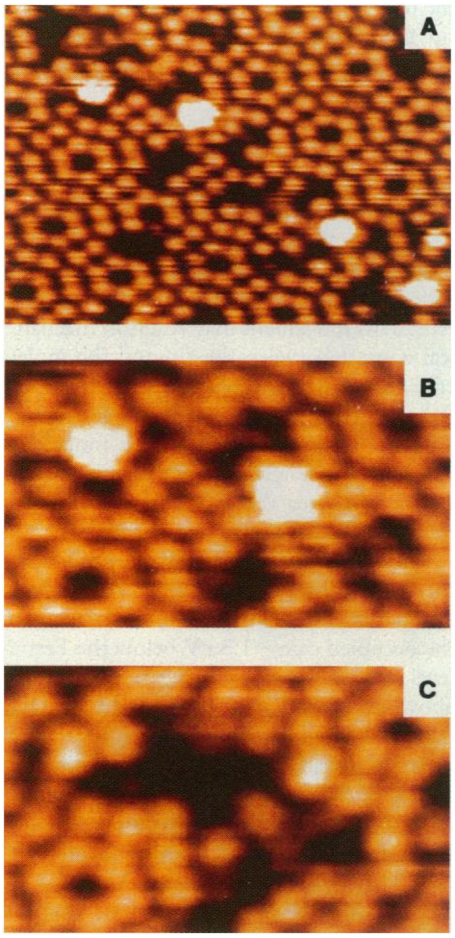

Fig. 3. (**A**) $B_{10}H_{14}$ molecules (large white spots) adsorbed along a domain boundary of the Si(111)-(7×7) surface. A number of dark defects are also present. (**B**) The two molecules on the upper left of (A) in a subsequent scan over a smaller area. (**C**) The result of electron bombardment at +8 V. The large molecules have dissociated to yield a number of new dark sites and some small bright features as fragments.

In a typical experiment, we imaged a region containing an adsorbed molecule at +2 V and 200 pA and then sent low-energy electrons to the sample by scanning the same region at an increased bias voltage. We then imaged again at +2 V to look for changes in the topography (*23*). When regions containing a molecule were scanned with bias voltages greater than $\sim$4 V, we observed several effects including displacement of adsorbed molecules, dissociation and fragmentation, and cluster formation. In contrast, no topographic changes were observed for regions containing only Si. Dissociation and fragmentation appear to be direct consequences of electron bombardment (see below). The formation of clusters occurred at higher surface coverages ($\geq$0.1 L) and involved groups of molecules adsorbed on large flat terraces of the (7 × 7) surface, rather than isolated molecules adsorbed near defects. The mechanism for cluster formation most likely involves the inhomogeneous electric field, which acts to draw molecules into the region under the tip (*4, 24*), together with possible electron-induced reactions.

Examples of dissociation and fragmentation are shown in Figs. 1 and 3. A region containing a $B_{10}H_{14}$ molecule adsorbed next to a surface defect was initially scanned at 200 pA and +2 V (Fig. 1B). This region was then subjected to a scan at 200 pA with the bias voltage increased to +8 V. During this scan, the tip retracted from the surface by $\approx$6 Å in order to maintain the set current. After the scan at +8 V, the region was imaged again at +2 V and 200 pA. Two distinct bright features appear in the resulting image (Fig. 1C) displaced with respect to the parent molecule (Fig. 1B). We argue that the presence of such spatially separated products is direct evidence of dissociation or fragmentation. Similar dissociation processes were observed for a number of adsorbed molecules after electron bombardment at +8 V bias, and no such processes were observed for regions containing only Si. We have not been able to specifically identify the fragments (*25*). To our knowledge, cracking patterns for the fragmentation of large boron hydride compounds by low-energy electrons are not available. At much higher electron energies ($\sim$70 eV), $B_{10}H_{14}$ is known to dissociate into a wide variety of fragments (*26*), with a propensity for the loss of hydrogen and zero to two boron atoms. The image in Fig. 1C appears to be consistent with such a "partial" dissociation process.

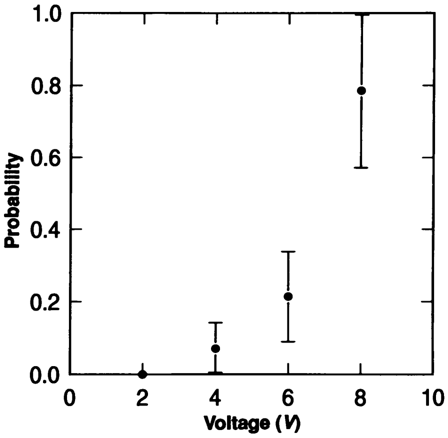

Fig. 4. The probability for dissociation is shown as a function of bias voltage. Error bars indicate uncertainties due to the finite number of samples.

Another mode of fragmentation is shown in Fig. 3. In this example, $B_{10}H_{14}$ molecules were initially adsorbed along a domain boundary (Fig. 3A). Two molecules from the upper left of this scan were selected and imaged at +2 V and 200 pA (Fig. 3B). The region containing these two molecules was scanned at +8 V and 200 pA and then imaged again at +2 V. After the scan at +8 V, no large molecular species were observed. Instead, there were many new dark sites in the region containing the original molecules and some small new bright features, which suggests extensive decomposition of the parent molecules. Fragmentation resulting in dark sites was observed frequently. The presence of dark sites qualitatively indicates that the Si dangling bonds that were initially present on the surface have been tied up by reactions with the decomposition products. Similar dark patches have been observed (*14*) upon thermal decomposition of $B_{10}H_{14}$. During the scan at +8 V, each atomic site receives a large dose of electrons with an effective kinetic energy in the range of 4 to 8 eV. Thus it is possible to dissociate the parent molecule with one electron and continue to further dissociate the fragments over the duration of the scan.

We examined the dependence of the various fragmentation processes on the applied bias voltage; Fig. 4 shows the net probability for partial or extensive dissociation due to a single scan over adsorbed molecules at 200 pA as a function of bias voltage. Occasional changes in the topography were observed for bias voltages as low as +4 V. When the voltage was increased to +8 V, the probability of inducing dissociation was quite high ($\sim$80%). A possible mechanism of dissociation by high electric fields is not likely since the fields in our case are $\leq$0.7 V/Å, a factor of $\sim$5 smaller than would be required for field dissociation (*27*). Also, in some experiments, the bias voltage was increased with a concurrent decrease in the stabilization current in order to maintain a constant electric field. Dissociation was observed only at high bias voltages. If the STM tip is brought into mechanical contact with the adsorbed molecule, then fragmentation can occur. We think that this process essentially involves severe local stress. However, under our typical conditions for recording images (+2 V bias, 200 pA), mechanical tip-molecule interactions are negligible, as evidenced by stable, reproducible images from scan to scan. Also, the tip retracts away from the surface as the voltage is increased from the normal scanning bias. Thus, we can rule out mechanical interactions with the tip as a dissociation mechanism during the scans at increased bias voltages. The evidence suggests that the observed dissociation processes are a direct consequence of the high flux of low-energy electrons incident on the adsorbed molecules.

REFERENCES AND NOTES

1. R. S. Becker, J. A. Golovchenko, B. S. Swartzentruber, *Nature* **325**, 419 (1987).
2. J. S. Foster *et al.*, *ibid.* **331**, 324 (1988).
3. D. M. Eigler and E. K. Schweizer, *ibid.* **344**, 524 (1990).
4. J. A. Stroscio and D. M. Eigler, *Science* **254**, 1319 (1991).
5. D. M. Eigler, C. P. Lutz, W. E. Rudge, *Nature* **352**, 600 (1991).
6. I.-W. Lyo and Ph. Avouris, *Science* **253**, 173 (1991).
7. See reports from STM 89 [*J. Vac. Sci. Technol. A* **8** (1990)] and STM 90 [*ibid.* **9** (1991)].
8. C. F. Quate, in *Proceedings of the NATO Science Forum '90*, L. Esaki, Ed. (Plenum, New York, in press).
9. R. S. Becker, G. S. Higashi, Y. J. Chabal, A. J. Becker, *Phys. Rev. Lett.* **65**, 1917 (1990).
10. C. R. K. Marrian, E. A. Dobisz, R. J. Colton, *J. Vac. Sci. Technol. A* **8**, 3563 (1990).
11. G. T. Furukawa and R. P. Park, *J. Res. Natl. Bur. Std.* **55**, 255 (1955).
12. Y. G. Kim, P. A. Dowben, J. T. Spencer, G. O. Ramseyer, *J. Vac. Sci. Technol. A* **7**, 2796 (1989).
13. Ph. Avouris, I.-W. Lyo, F. Bozso, E. Kaxiras, *ibid.* **8**, 3405 (1990).
14. Ph. Avouris, *J. Phys. Chem.* **94**, 2246 (1990).
15. R. A. Rosenberg *et al.*, *Appl. Phys. Lett.* **58**, 607 (1991).
16. F. K. Perkins, R. A. Rosenberg, S. Lee, P. A. Dowben, *J. Appl. Phys.* **69**, 4103 (1991).
17. Ph. Avouris and R. Wolkow, *Phys. Rev. B* **39**, 509 (1989).
18. J. Tersoff and D. R. Hamann, *ibid.* **31**, 805 (1985).
19. T. Klitsner *et al.*, *ibid.* **41**, 3837 (1990).
20. N. D. Lang, *ibid.* **34**, 5947 (1986).
21. See L. A. Laws, R. M. Stevens, W. N. Lipscomb, *J. Am. Chem. Soc.* **94**, 4467 (1972).
22. S. G. Shore, in *Boron Hydride Chemistry*, E. L. Muetterties, Ed. (Academic Press, New York, 1975), chap. 3.
23. A clean tip, that is, one that does not deposit material onto the sample surface when the bias voltage is increased, is essential. The tip had to be cleaned by electron bombardment at ~10 nA and −10 V for a few minutes prior to imaging $B_{10}H_{14}$ molecules.
24. L. J. Whitman, J. A. Stroscio, R. A. Dragoset, R. J. Celotta, *Science* **251**, 1206 (1991).
25. In interpreting topographic images of the dissociation products, one should keep in mind that these reflect a combination of geometric and electronic structures.
26. A. Quayle, *J. Appl. Chem. (London)* **9**, 395 (1959).
27. T. T. Tsong, *Atom-Probe Field Ion Microscopy* (Cambridge Univ. Press, Cambridge, 1990).

28. We thank P. Dowben of Syracuse University for providing high-purity samples of $B_{10}H_{14}$ and I.-W. Lyo for invaluable technical help.

29 October 1991; accepted 7 January 1992

C_{60} Rotation in the Solid State: Dynamics of a Faceted Spherical Top

ROBERT D. JOHNSON,* COSTANTINO S. YANNONI, HARRY C. DORN,†
JESSE R. SALEM, DONALD S. BETHUNE

The rotational dynamics of C_{60} in the solid state have been investigated with carbon-13 nuclear magnetic resonance (^{13}C NMR). The relaxation rate due to chemical shift anisotropy ($1/9T_1^{\mathrm{CSA}}$) was precisely measured from the magnetic field dependence of T_1, allowing the molecular reorientational correlation time, τ, to be determined. At 283 kelvin, $\tau = 9.1$ picoseconds; with the assumption of diffusional reorientation this implies a rotational diffusion constant $D = 1.8 \times 10^{10}$ per second. This reorientation time is only three times as long as the calculated τ for free rotation and is shorter than the value measured for C_{60} in solution (15.5 picoseconds). Below 260 kelvin a second phase with a much longer reorientation time was observed, consistent with recent reports of an orientational phase transition in solid C_{60}. In both phases τ showed Arrhenius behavior, with apparent activation energies of 1.4 and 4.2 kilocalories per mole for the high-temperature (rotator) and low-temperature (ratchet) phases, respectively. The results parallel those found for adamantane.

THE FACT THAT C_{60} MOLECULES IN the solid state interact only weakly leads to interesting dynamical behavior. Rotational dynamics of molecules in condensed phases can be probed with NMR spectroscopy. In earlier NMR studies of solid C_{60} (*1, 2*), it was found that the spectrum at ambient temperature consists of a relatively narrow line rather than a broad powder pattern, as expected for randomly oriented stationary molecules. This sharp spectrum implies rapid isotropic molecular reorientation. Powder patterns reflect the variation in the magnetic shielding of a nucleus with molecular orientation (chemical shift anisotropy or CSA). Below 100 K the reorientation rate slows sufficiently to allow determination of the chemical shift tensor elements from the shape of the NMR line (*1*).

The molecular reorientation time τ can be found from measurements of the spin lattice relaxation time, T_1, because for rotating molecules, anisotropic shielding leads to fluctuating fields proportional to the external magnetic field (B_0), with a concomitant relaxation rate proportional to B_0^2. The CSA relaxation mechanism is expected to dominate in both liquids and solids at sufficiently high fields. A classic T_1 minimum was observed at 233 K in the first relaxation measurements on solid C_{60}. Interpreting this in terms of CSA relaxation yielded a value of τ = 2.1 ns at this temperature (*1*).

More recently, Heiney *et al.* (*3*) found from x-ray studies and calorimetry that solid C_{60} exhibits a phase transition near 249 K from a simple cubic structure at low temperatures to a face-centered-cubic (FCC) structure. This transition was examined with NMR by Tycko *et al.* (*4*), who found a break in the T_1 relaxation rate at 260 K. These studies suggest that the phase above the transition temperature is characterized by free rotation or rotational diffusion and that the phase below the transition is characterized by jump rotational diffusion between symmetry-equivalent orientations.

In this report we present detailed measurements of the reorientational correlation time τ for solid C_{60} over the temperature range 240 to 331 K. The quantity τ was calculated from the CSA relaxation rate and the measured chemical shift tensor elements. Because the CSA relaxation rate has a unique quadratic dependence on magnetic field, measurement of T_1 as a function of magnetic field allows the CSA contribution to be obtained and separated from non-CSA (NCSA) relaxation mechanisms. Results were obtained both above and below the phase transition, which we found at 260 K

IBM Research Division, Almaden Research Center, 650 Harry Road, San Jose, CA 95120–6099.

*To whom correspondence should be addressed.
†Permanent address: Department of Chemistry, Virginia Polytechnic Institute and State University, Blacksburg, VA 24061.